Deuteron Stripping on Ca^{46} at 10-MeV Bombarding Energy

J. H. BJERREGAARD, OLE HANSEN, AND G. SIDENIUS
Institute for Theoretical Physics, University of Copenhagen, Copenhagen, Denmark
(Received 28 January 1965)

The reaction $Ca^{46}(d,p)$ was examined at 10.129-MeV bombarding energy with an energy resolution of 15 keV. Absolute differential cross sections were measured at 24 scattering angles. The target was prepared by isotope separation to a relative purity in Ca^{46} of more than 99%. Twenty-eight levels in Ca^{47} up to 6.6-MeV excitation were identified. Twenty-one of the transitions could be analyzed by deuteron-stripping theory in the distorted-wave approximation to yield values of the orbital angular momentum of the transferred neutron and of the transition strength. Spin values are suggested for a number of Ca^{47} levels, partly based on the back-angle behavior of the $l_n=1$ transitions and partly on shell-model systematics. The data are discussed in terms of shell-model sum rules and comparisons between the present data and other data on Ca^{47}, as well as on other $N=27$ nuclei, are presented.

I. INTRODUCTION

CALCIUM[47] consists of 20 protons and 27 neutrons and should, thus, have a ground-state configuration of one $f_{7/2}$ neutron hole in a Ca^{48} core. Two low-lying states in Ca^{47} have been observed in the decay[1] of K^{47}. The (p,d) reaction on Ca^{48} has recently been studied by Kashy *et al.*[2] revealing states in Ca^{47} up to an excitation energy of 2.6 MeV. The pickup spectrum, as observed, is quite simple and supports the one-neutron hole character of most of the states excited. The present experiment on the $Ca^{46}(d,p)Ca^{47}$ reaction emphasizes those levels in Ca^{47} that are describable as a neutron outside a Ca^{46} core; that is, the two-hole, one-particle states relative to a Ca^{48} core. Thus, it provides an essentially different picture of the Ca^{47} level scheme.

Twenty-eight levels were observed in Ca^{47} up to an excitation energy of 6.6 MeV. The distorted-wave (DW) analysis of the measured cross sections suggests that all of the $1f_{7/2}$, $2p_{3/2}$, and $2p_{1/2}$ strengths allowed by the shell-model sum rules[3] have been observed. In addition, part of the $1f_{5/2}$ and $1g_{9/2}$ strengths were found, whereas none of the $3s_{1/2}$ or $2d_{5/2}$ states were identified.

A low-lying state at 2.606 MeV has $l_n=0$ character, but it is weak. It coincides energetically with a $l_n=0$ pickup state[2] and thus probably shows that a small fraction of the $2s_{1/2}$ shell-model orbit is not occupied in the Ca^{46} ground state.

Three of the $l_n=1$ distributions show a sharp minimum ("dip") in the backward quadrant, which has been shown by Lee and Schiffer[4] to be characteristic for $2p_{1/2}$ (d,p) transitions. The positions of the observed dips in the present case depend on the Q value.

Section II of this report covers the experimental techniques, the results, and the DW analysis. Section III contains a sum-rule analysis of our experimental results, a discussion of the ground-state $Ca^{46}(d,p)Ca^{47}$ Q value, and finally a comparison of the present data with other data on Ca^{47} and with data on the $N=27$ nuclei Ti^{49} and Cr^{51}. The influence of the proximity of the doubly closed shell nucleus Ca^{48} to Ca^{46} and Ca^{47} is investigated in some detail.

II. EXPERIMENTAL TECHNIQUES, ANALYSIS, AND RESULTS

1. Targets

The natural relative abundance of Ca^{46} is 0.0033%, so that the fabrication of a useful Ca^{46} target constitutes a major difficulty. The target problem was solved by adapting an isotope reseparation technique developed in connection with Coulomb-excitation experiments from rare-earth isotopes of low natural abundance.[5]

The ion source of the Copenhagen isotope separator was charged with 4 mg of $CaCO_3$ obtained from Oak Ridge National Laboratory and enriched to 9% in Ca^{46}. In order to ensure maximum collection efficiency, the "retardation method" was employed.[6] Before impinging upon the 50–75 $\mu g/cm^2$ carbon backings, the 50 keV Ca^+ ions are retarded to about 0.8 keV, and the beam is simultaneously bent and focused by means of an electrostatic lens. The bending of the beam is essential to prevent energetic neutral Ca^{46} atoms from hitting and damaging the carbon backings. Neutral atoms are formed by charge exchange with the residual gas in the collector chamber of the isotope separator. The Ca spot on the carbon backing was approximately 0.3×2 mm^2. The separator ion-source conditions were tested on natural calcium. The highest separation efficiency (about 15%) was obtained by passing a stream of CCl_4 through the $CaCO_3$ which was placed in an oven at a temperature of about 900°C. $CaCl_2$ evaporates from the oven directly into the ion source. The CCl_4 stream was found to attack the quartz insulators of the ion source to some extent.

Two Ca^{46} targets were manufactured, each of an approximate thickness of 20 $\mu g/cm^2$ in Ca^{46}, each con-

[1] T. Kuaroyanagi, T. Tamura, K. Tanaka, and H. Morinaga, Nucl. Phys. **50**, 417 (1964).
[2] B. F. Bayman, T. W. Conlon, and E. Kashy (to be published).
[12] T. A. Belote and J. Rapaport (private communication).
[3] M. H. Macfarlane and J. B. French, Rev. Mod. Phys. **32**, 567 (1960).
[4] L. L. Lee and J. P. Schiffer, Phys. Rev. **136**, B405 (1964).
[5] J. H. Bjerregaard, B. Elbek, O. Hansen, and P. Salling, Nucl. Phys. 44, 280 (1963).
[6] G. Sidenius and O. Skilbried, in *E.M. Separation of Radioactive Isotopes* (Springer-Verlag, Vienna, 1961), pp. 234 and 243.

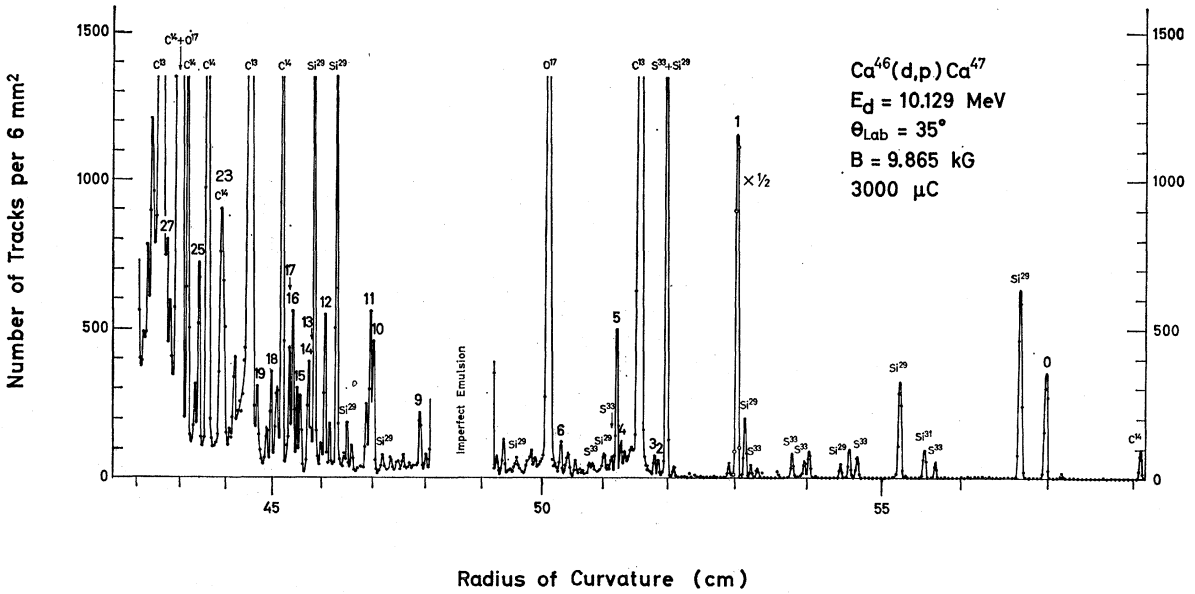

FIG. 1. Proton spectrum obtained at 35° laboratory angle. The plates were scanned in $\frac{1}{4}$-mm strips across the exposed zone; the ordinate used in the figure represents a summation over four strips. The excitation energies of Table I derive (whenever possible) from position determinations of the proton peaks at this angle. Proton groups belonging to mass 47 are marked by numbers 0 through 27 in correspondence with the level numbers used in Table I. Impurities were not identified systematically, since the target composition is known from previous experiments (Ref. 8). A number of impurity groups are marked by the chemical symbol and mass number of the residual nucleus. The positions of these groups were used as a check on the Q-value scale. Because of the complexity of the proton spectrum it is possible that weak groups belonging to mass 47 may have been missed.

taining about 10 μg/cm^2 of Si^{28} (collection of $H_2{}^1Si^{28}O^{16}$ which has mass 46), some Si^{30} (collection of $Si^{30}O^{16}$), and 1 to 2 μg/cm^2 of Cl (probably from diffusion from the ion source where CCl_4 was applied).

The Ca^{46} enrichment was judged from the mass spectrum observed on the beam-scanning system[7] of the isotope separator to be better than 99%. No particle groups belonging to other calcium isotopes were observed from the (p,p), (p,p'), (d,d), (d,d'), and (d,p) reactions investigated (see also Ref. 8).

2. The $Ca^{46}(d,p)$ Experiment, Procedures, and Results

The deuteron elastic-scattering experiment has been described previously.[8] The experimental setup for the (d,p) experiment is identical to that used for previous experiments on the calcium isotopes.[8,9]

A Ca^{46} target was bombarded with 10.129-MeV deuterons from the Aldermaston tandem electrostatic generator. The reaction products were momentum analyzed at 24 scattering angles in the multiple-gap, broad-range, heavy-particle spectrograph of Middleton and Hinds,[10] and the protons were recorded on nuclear-track plates, the emulsions of which were covered by polyethylene foils thick enough to stop all other heavy, charged particles. The over-all energy resolution was 15 keV, and the exposure was 3000 μC.

Since the Ca^{46} (d,p) ground-state Q value has not been reported previously, two extra (d,p) experiments were performed at the Copenhagen 4-MV electrostatic generator and single-gap spectrograph with the specific purpose of determining this Q value. The experimental procedures and the spectrograph calibration were identical to those employed by Bjerregaard *et al.*[11] The two Q values determined from the 4-MeV experiment and that found in the 10-MeV experiment agreed to within 4 keV, resulting in a value of 5052±8 keV.

Part of a Ca^{46} $(d,p)Ca^{47}$ spectrum is shown in Fig. 1. The presence of silicon and chlorine complicates the spectrum and its analysis. Moreover, since the Aldermaston spectrograph is not energy calibrated at back angles, we found it impossible to identify the proton groups for scattering angles larger than 90° at Ca^{47} excitation energies above 4.4 MeV. At Ca^{47} excitations higher than 6.07 MeV we found it impossible to extract reliable yields, and above 6.6 MeV the density of proton groups on the plates prohibited the further analysis of the data.

Because of these conditions, it would seem desirable to repeat the $Ca^{46}(d,p)$ experiment at another bombarding energy. This has in fact been done[12] at the High

[7] K. O. Nielsen and O. Skilbreid, Nucl. Instr. Methods **1**, 159 (1957).
[8] T. A. Belote, J. H. Bjerregaard, O. Hansen, and G. R. Satchler, Phys. Rev. (to be published).
[9] J. H. Bjerregaard, H. R. Blieden, O. Hansen, G. Sidenius, and G. R. Satchler, Phys. Rev. **136**, B1348 (1964).
[10] R. Middleton and S. Hinds, Nucl. Phys. **34**, 404 (1962).
[11] J. H. Bjerregaard, P. F. Dahl, O. Hansen, and G. Sidenius, Nucl. Phys. **51**, 641 (1964).
[12] T. A. Belote and J. Rapaport (private communication).

TABLE I. $Ca^{46}(d,p)Ca^{47}$ results. $Q_0=5052\pm8$ keV.

Level No.	Excitation energy (keV±10)	Transition strength[a] $l=0$	$l=1$	$l=2$	$l=3$	$l=4$	j,π	Comments
0	0	...	...	...	2.20[b]	...	$7/2^-$	
1	2013	...	3.30	...	...	...	$3/2^-$	No back dip
2	2579	...	...	...	...	...	...	Nonstripping
3	2606	0.04	...	...	...	...	$1/2^+$	Assuming $2s_{1/2}$
4	2857	...	0.08	...	...	...	$1/2^-$	Dip at 135°
5	2878	...	0.49	...	...	...	$1/2^-$	Dip at 145°
6	3301	...	...	...	...	...	...	Nonstripping
7	4012	...	0.52	...	...	...	$3/2^-$	No back dip
8	4049	...	0.99	...	...	...	$1/2^-$	Dip at 155°
9	4403	...	0.05	...	...	...	$3/2, 1/2^-$	No back-angle data
10	4782	...	...	...	0.79	...	$5/2^-$	
11	4804	...	0.26	...	...	...	$3/2, 1/2^-$	No back-angle data
12	5192	...	0.22	...	...	...	$3/2, 1/2^-$	No back-angle data
13	5311	...	...	(0.04)	0.18	...	$5/2^{(-)}$	
14	5328	...	...	...	...	0.93	$9/2^+$	
15	5428	...	...	(0.06)	0.29	...	$5/2^{(-)}$	
16	5453	...	...	...	...	...	...	
17	5478	...	0.08	...	...	...	$3/2, 1/2^-$	No back-angle data
18	5636	...	...	(0.11)	0.36	...	$5/2^{(-)}$	
19	5761	...	0.08	...	...	...	$3/2, 1/2^-$	No back-angle data
20	5807	...	...	(0.12)	0.59	...	$5/2^{(-)}$	
21	5842	...	...	...	...	1.02	$9/2^+$	
22	5874	...	0.04	...	...	...	$3/2, 1/2^-$	No back-angle data
23	6066	...	...	(0.12)	0.58	...	$5/2^{(-)}$	
24	6191	...	...	...	...	...	...	
25	6270	...	...	...	...	...	...	
26	6366	...	...	...	...	...	...	
27	6555	...	...	...	...	...	...	

[a] Defined as $(2j+1)S_{lj}$, j being the final state spin, l the l_n-value and S the spectroscopic factor. The uncertainty in the experimental cross-section scale is ±25%. The reliability of the DW calculations is discussed in the text. The X potential and no cutoff was used.
[b] Average of lower cutoff radius equals 4.6 F and no cutoff, with X potential.

Voltage Laboratory of MIT from the second of our Ca^{46} targets.

An absolute cross-section scale was established for the present experiment, in which the elastic deuteron scattering was not recorded, by assuming that the differential cross sections for the (d,p) transitions to the Ca^{47} ground and first excited states are identical at 10.129 MeV (the bombarding energy used in the present experiment) and at 10.005 MeV (the bombarding energy of the (d,d') experiment[8]). The normalization of the two experiments was done on the proton groups leading to $Ca^{47}(0)$ and $Ca^{47}(1)$ at scattering angles around the maximum of the former. The standard deviation from the mean on eight determinations of the (d,p) yield ratio between the two experiments was ±5%.

The Ca^{47} excitation energies, as determined in the multiple-gap experiment, are given in Column 2 of Table I. The values for states (1) and (5) checked well with those obtained from the Copenhagen 4-MeV experiment. The observed angular distributions are shown in Figs. 2 and 3, in comparison with DW predictions.

3. Distorted-Wave Analysis

The optical-model analysis of the $Ca^{46}(d,d)$ data has been described previously.[8] Both X and Y potentials of that reference (see also Table II) where used in the present work to generate (d,p) differential cross sections from DW calculations. The proton potential employed was taken from the work of Perey[13]; its parameters are given in Table II. Also shown are the parameters used for the captured neutron. A binding energy of the captured neutron equal to its experimental separation energy $Q+2.23$ MeV was assumed. The DW calculations were performed for a number of Q values between 5.05 and -1 MeV covering the $2s$, $3s$, $2p$, $1f$, $2d$, and $1g$ shell-model states for the captured neutron.

A lower cutoff could be inserted into the radial integrals of the DW calculations. Predictions were obtained with a cutoff at 4.6 F. The changes in the predicted angular distributions with variation of deuteron potential and cutoff radius in general are negligible compared with the experimental uncertainties. An exception to this rule is the ground-state transition which has the largest Q value (see, for example, Fig. 2). Shape-

TABLE II. Optical-model parameters.

Particle	Potential	V (MeV)	r_0 (F)	a (F)	W_D (MeV)	r_0' (F)	a' (F)	r_c (F)
d	X	115.0	1.0	0.804	13.0	1.419	0.660	1.30
d	Y	160.1	0.769	0.933	12.4	1.488	0.648	1.30
p		52.0	1.25	0.650	11.0	1.25	0.470	1.25
n		[a]	1.25	0.650				

[a] V adjusted to give the neutron a binding energy equal to the observed separation energy ($Q_{d,p}+2.23$ MeV).

[13] F. G. Perey, Phys. Rev. **131**, 745 (1963).

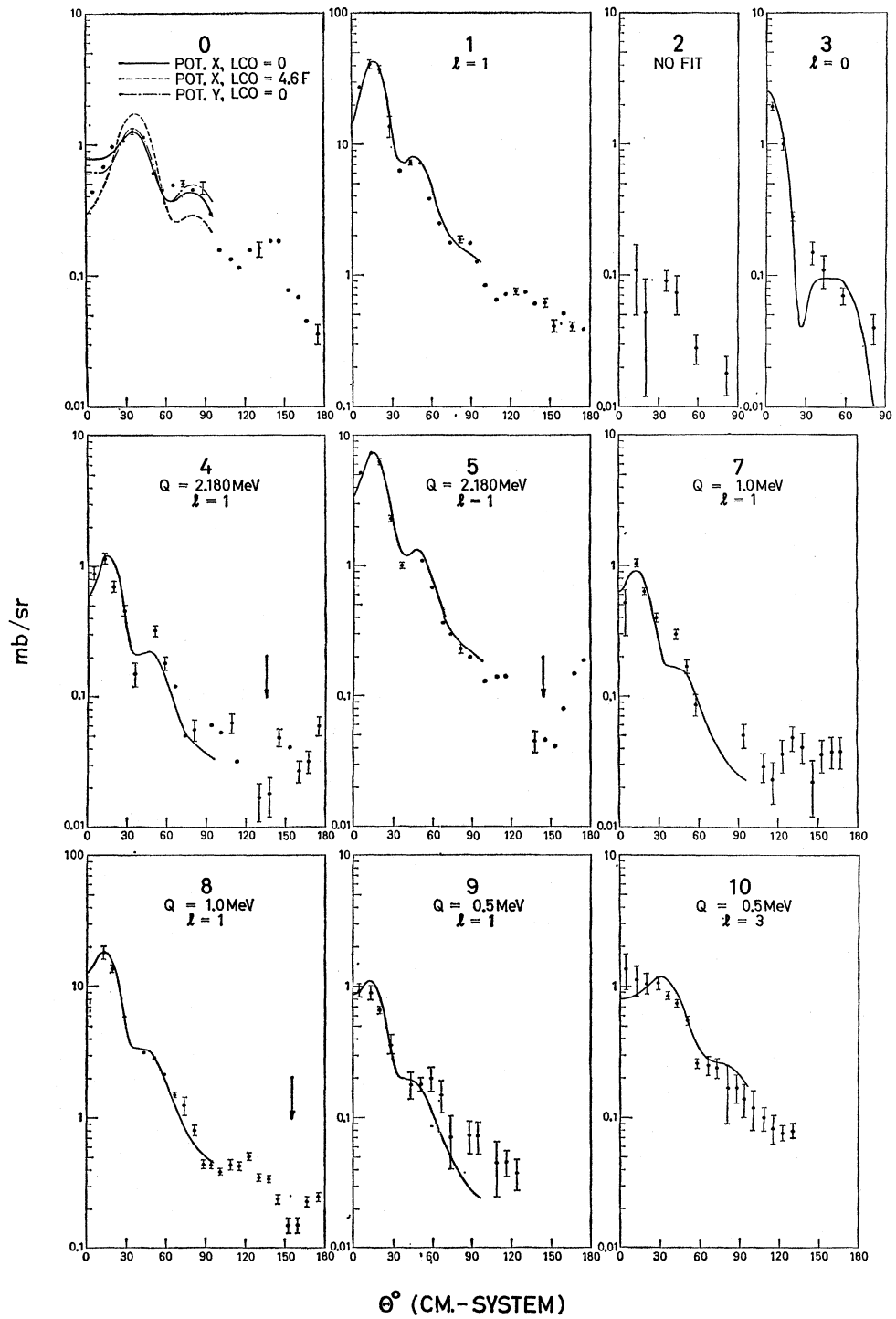

FIG. 2. $Ca^{46}(d,p)Ca^{47}$ angular distributions. Experimental points are marked by filled circles. Typical errors are indicated by vertical bars. The different distributions are identified by a number shown in the top center of each figure; this number corresponds to the level numbers of Table I and of Fig. 1. The curves are distorted-wave predictions obtained as described in the text. The Q value used for the DW calculation is displayed if it differs from the experimental Q value. Except when otherwise stated, the X-deuteron potential (Table II) with no cutoff was used. The value assumed for the orbital angular momentum of the captured neutron (l_n value) is indicated for each curve. The calculated curves were normalized to experiment as described in the text. In the cases of transitions (4), (5) and (8) the backward "dip" (see text) is indicated by an arrow.

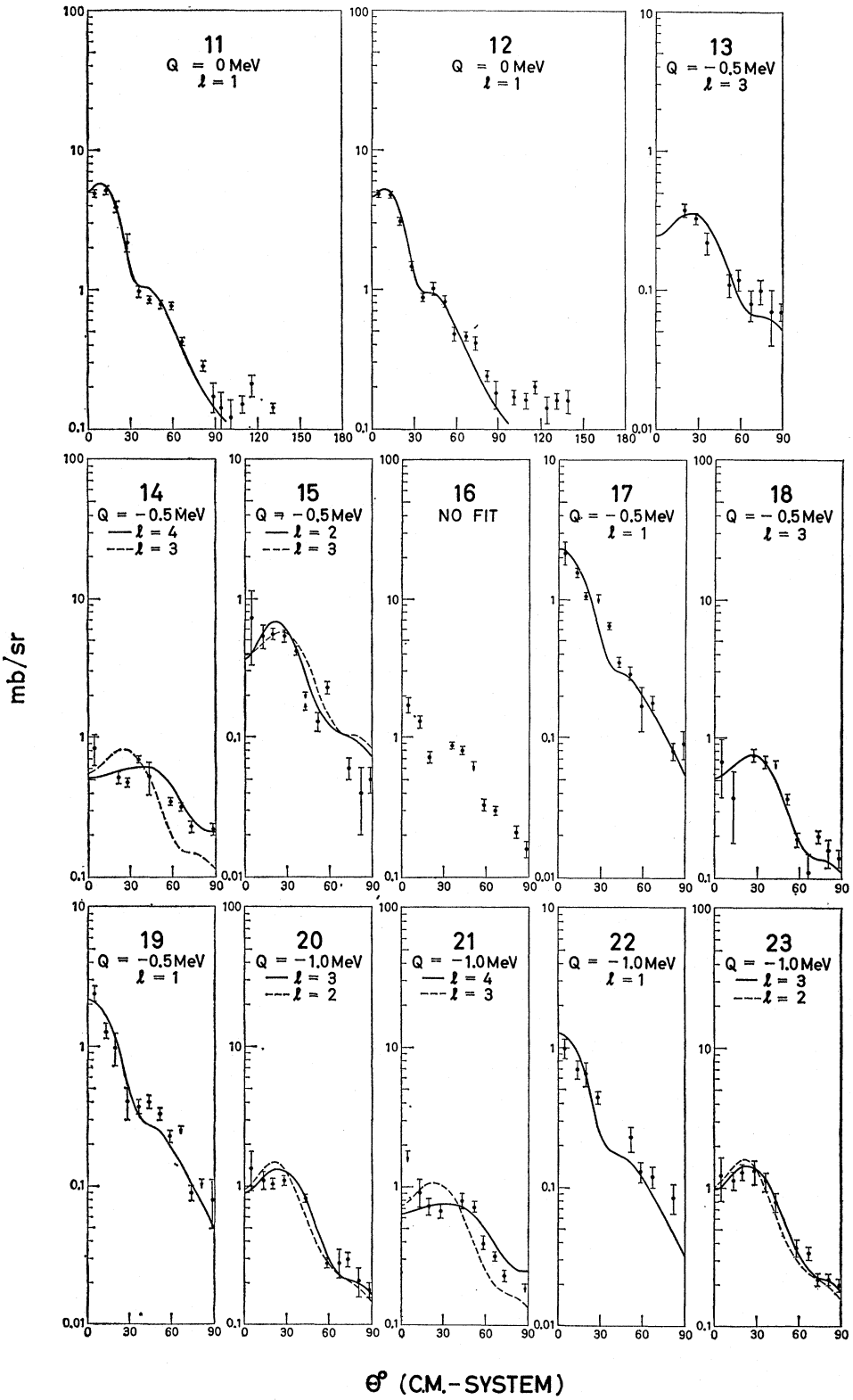

FIG. 3. $Ca^{46}(d,p)Ca^{47}$ angular distributions. See caption, Fig. 2.

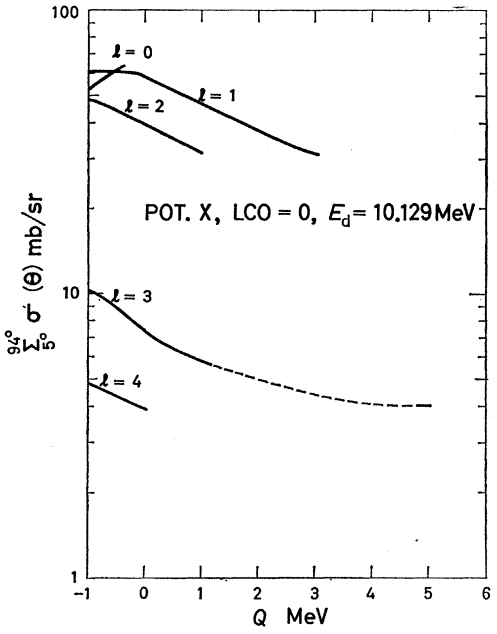

FIG. 4. Summed DW cross sections versus Q value. The sum extends over center-of-mass angles corresponding to laboratory angles between 5° and 87.5° in steps of 7.5° plus the angle of 92.5°. These graphs were used for interpolation in Q value when obtaining the transition strengths given in Table I. DW calculations from the deuteron X potential (Table II) and no cutoff were used.

wise, this distribution may be fitted very well with either deuteron potential; the zero-cutoff curves give somewhat better agreement than those for a cutoff at 4.6 F. However, the spectroscopic factors derived from the four different predictions vary inside a factor of 2. The value given in Table I is the average of those obtained using no cutoff and a cutoff at 4.6 F with the X potential. This seems reasonable; it is difficult to justify a sharp cutoff, but there are several reasons (such as nonlocality and finite-range effects) which reduce the contributions from the nuclear interior.[14] The result of including these is generally intermediate between the effects of no cutoff and a cutoff near the nuclear surface. In all other cases the spectroscopic factors, as derived from the different predictions, vary by less than about 10% for $l_n=1$ and 3 and less than 20% for $l_n=2$ and 4 For definiteness, we have used potential X with no cutoff.

The spectroscopic strengths $[(2j+1)S_{lj}]$ given in Table I were obtained by comparing the observed differential cross sections summed over the forward quadrant of scattering angles to the corresponding cross-section sum, as predicted by the DW calculation. Interpolation in Q was made by means of the graphs presented in Fig. 4.

As shown by the DW angular distributions given in Fig. 5, the curves for $l_n=2$ and 3 are quite similar, thus making it difficult to decide whether an experimental distribution corresponds to $l_n=2$ or 3. This ambiguity exists for excitation energies above 5 MeV. In all relevant cases, $l_n=3$ gives marginally the better fit to experiment (see Figs. 2 and 3), but the data do not allow a definite assignment. Table I therefore quotes both an $l_n=2$ and an $l_n=3$ strength in those cases. From the shell-model systematics, $l_n=3$ is the more likely assignment. It is hoped that the 7-MeV data[12] will clarify this point.

The omission in the DW calculations of finite-range and spin-orbit effects will influence the spectroscopic strengths derived from the present data. It was found in the $Ca^{40}(d,p)$ study of Lee *et al.*[14] that, at 11-MeV bombarding energy, the inclusion of finite-range effects changed the predicted $l_n=3$, $Q=6.14$-MeV (d,p) cross section towards lower values by some 35% relative to the zero-range prediction. The spin-orbit effect on the other hand *increases* the cross section by a similar amount for a $1f_{7/2}$ neutron transfer. Thus, the two effects tend to compensate each other for the transfer of an $f_{7/2}$ neutron. Since the spin-orbit effect has the opposite direction for an $f_{5/2}$ neutron transition, the two effects in this case add together. The effects for $2p$ transitions are smaller (less than 10%). These results are typical of nuclei in this mass region and at this energy. Other calculations show that $1g$ capture is affected in a way similar to $1f$, except that the spin-orbit effect is somewhat larger. The influence of these effects in the present case is significant only for the $1f_{5/2}$ transitions, the strengths of which may be quoted about 50% low in Table I.

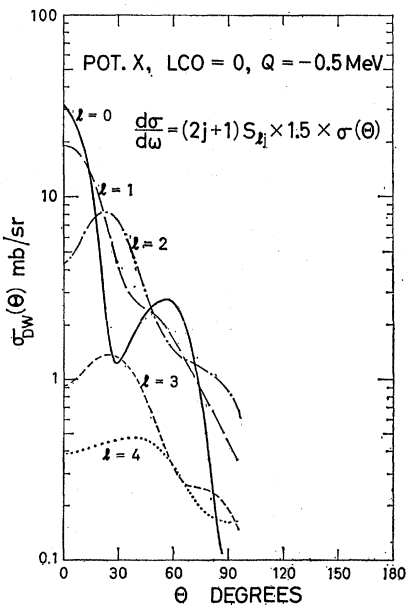

FIG. 5. Typical angular distributions as predicted by the DW calculations. The figure illustrates the accidential similarity between the $l_n=2$ and $l_n=3$ distributions at these Q values. There is no difficulty in distinguishing other l_n values from one another.

[14] L. L. Lee, J. P. Schiffer, B. Zeidman, G. R. Satchler, R. M. Drisko, and R. H. Bassel, Phys. Rev. 136, B971 (1964).

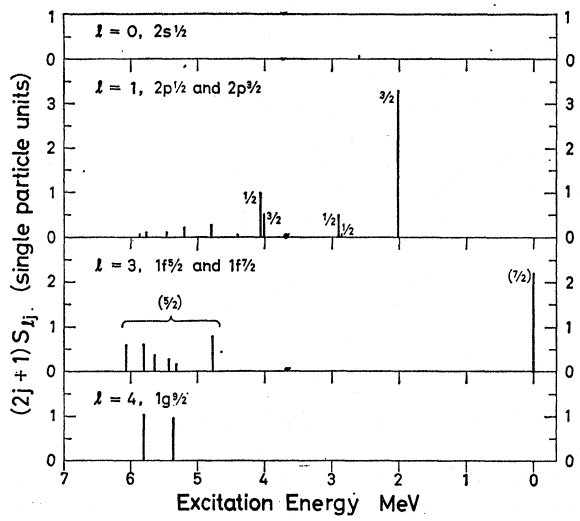

FIG. 6. Ca^{47} strength function. The (d,p) strengths of Table I plotted against excitation energy.

The last column of Table I gives a number of comments on the observed angular distributions, mostly relating to the spin assignments suggested in column 8. The terms "no dip" or "dip" refer to the back-angle behavior of the $l_n=1$ distributions. As discovered by Lee and Schiffer,[4] a sharp relative minimum ("dip") occurs at back angles for $2p_{1/2}$ transitions but not for $2p_{3/2}$ transitions. Our assignments of spins $\frac{1}{2}$ and $\frac{3}{2}$ are based solely on this back-angle behavior. In the 7-MeV data on $Ca^{46}(d,p)$ (Ref. 12) "dips" were also observed for transitions (11) and (12), which therefore probably are $p_{1/2}$ transitions. The differentiation between spins $\frac{7}{2}$ and $\frac{5}{2}$ is made on grounds of shell-model systematics and from the observed strength function (see Sec. III.1).

III. DISCUSSION

1. Strength Function and Sum-Rule Analysis

Figure 6 shows the observed transition strengths $(2j+1)S_{lj}$ of Table I plotted versus excitation energy.

The $l_n=3$ strength splits into two distinct groups, the ground-state transition and the transitions above 4.8-MeV excitation energy. We believe this grouping to mean that different final states are involved; that is, $\frac{7}{2}$ for the ground state and $\frac{5}{2}$ for the higher lying group. Corresponding splitting of the $l_n=3$ strength function has also been observed in neighboring nuclei (see, for example, Refs. 15 and 16).

The $l_n=1$ strength is distributed over the entire region of excitation observed, although the weakness of the high-excitation transitions may indicate that most of the available $2p$ strength has been used up at these energies.

[15] P. D. Barnes, C. K. Bockelman, O. Hansen, and A. Sperduto, Phys. Rev. **138**, B597 (1965) [$Ti^{47}(d,p)Ti^{48}$] and (unpublished) [$Ti^{49}(d,p)Te^{50}$].

[16] T. A. Belote, A. Sperduto, and W. W. Buechner, Phys. Rev. (to be published) [$Ca^{40}(d,p)Ca^{41}$].

The lack of low-lying $l_n=2$ transitions shows that the $1d$ orbitals are mostly occupied in the Ca^{46} ground state. The single, weak, low-lying $l_n=0$ transition (level 3) indicates that also the $2s$ orbits are practically occupied.

The observed transition strengths may be analyzed quantitatively in terms of the two shell-model sum rules[3,17]:

$$(1/(2J_i+1))\sum_a(2J_f+1)S^a{}_{lj}=\text{number of } (l,j) \text{ neutron holes in the target;} \quad (1)$$

$$E'_{lj}\sum_a S^a{}_{lj}=\sum_a E^a{}_{lj}S^a{}_{lj}. \quad (2)$$

Here, J_i designates the target spin ($J_i=0$) and J_f the final state spin. $S^a{}_{lj}$ is the spectroscopic factor for the ath level corresponding to the transfer of a neutron of $l_n=l$ and spin j ($J_f=j$, in the present case). E is the experimental excitation energy and E' the "single-particle excitation energy in the limit of zero residual interaction strength."[17]

Since no information has been published on pickup experiments on Ca^{46}, we have no measure of the possible $(2p_{3/2})^2$ admixtures in the target ground state of the present experiment. (p,d) reactions from even calcium and titanium isotopes[2,18] all reveal such admixtures but of quite low strengths (≈ 0.2 particles). We may therefore expect the right-hand side of sum rule (1) to equal 2 ± 0.2 for the $f_{7/2}$ transitions and 6 ∓ 0.2 for the $(p_{3/2}+p_{1/2})$ transitions in the present case.

All of the $Ca^{46}(d,p)$ $1f_{7/2}$ strength is collected in the ground-state transition (Fig. 6) and the observed $(2j+1)S_{lj}$ agrees well with the sum-rule limit (see Table III). Similarly, good agreement is also found for the $2p_{3/2}$, $2p_{1/2}$, and $(2p_{1/2}+2p_{3/2})$ cases (Table III).

We therefore conclude that (a) the DW analysis of the $Ca^{46}(d,p)$ cross sections is reasonable and (b) the Ca^{47} ground state has true single-particle structure. The latter conclusion is supported by the $Ca^{48}(p,d)$ results.[2]

The observed $1f_{5/2}$ and $1g_{9/2}$ strengths reveal, when compared to the sum-rule limits (Table III), that only a portion of these transitions has been found.

The energy-weighted sum rule (2) may be used to derive the parameter E'_{lj} from experiment. Since E'_{lj} measures the unperturbed single-particle energies, the

TABLE III. Sum-rule limits in $Ca^{46}(d,p)Ca^{47}$.

	$\Sigma_a(2j+1)S^a{}_{lj}$					
Shell-model state	$1f_{7/2}$	$2p_{3/2}$[a]	$2p_{1/2}$[b]	$p_{3/2}+p_{1/2}$[c]	$1f_{5/2}$	$1g_{9/2}$
Experimental	2.20	3.82	1.56	6.11	2.79	1.95
Theoretical	2	4	2	6	6	10

[a] Includes such $l=1$ transitions for which the angular distributions at back angles are observed to show no dip.
[b] Includes such $l=1$ transitions for which the angular distributions are observed to have a dip at back angles.
[c] Includes all $l=1$ transitions observed.

[17] S. Yoshida, Nucl. Phys. 38, 380 (1962).

[18] E. Kashy and T. W. Conlon, Phys. Rev. **135**, B389 (1964).

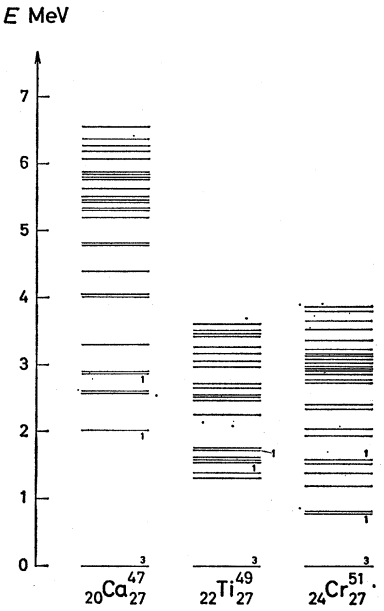

FIG. 7. Level schemes for Ca^{47}, Ti^{49}, and Cr^{51}. The two lowest strong $l_n=1$ transitions are marked on each level scheme. References for the data used in the figure are given in the text.

spread around E'_{lj} of the measured E_{lj} indicates the strength of the residual interactions. Presently, the E'_{lj} values were derived from the data of Table I and the extra spin assignments of Ref. 12. Since some $l_n=1$ transitions have not been assigned a spin, an ambiguity exists in the $E'_{1,1\pm1/2}$. The $E'_{1,3/2}$, say, was determined as $\frac{1}{2}(E'_{+}+E'_{-})$, where E'_{+} included levels (17), (19), and (22), and E'_{-} did not. The experimental numbers given in Table IV are the separation energies (B'_{lj}) defined as $B'_{lj}=Q_{0(d,p)}+2225-E'_{lj}$(keV). The uncertainties given for $l_n=1$ are $\frac{1}{2}|B'_{+}-B'_{-}|$. It may be remarked that the B'_{lj} values derived from experiment do not depend on the absolute values of the S_{lj}. Also given in Table IV are the B'_{lj} inferred from the shell-model systematics as given in Ref. 19. It is seen that the present data fit into the systematics fairly well. The value of $E'_{1,1/2}-E'_{1,3/2}$ for Ca^{47} is 1.67 ± 0.15 MeV (Table IV); that is, less than observed for Ca^{49} (2.03 MeV, Ref. 20) and Ca^{41} (2.04 MeV, Ref. 16) but larger than found for Ti^{51} (1.37 MeV, Ref. 21). The fractionating of the p strength in Ca^{47} is greater than found in Ca^{49} (no fractionation) and in Ti^{51}, but smaller than observed in Ca^{41}.

TABLE IV. Unperturbed single-particle binding energies[a] (MeV).

Configuration	Present experiment	Ref. 19
$1f_{7/2}$	7.28	9.5
$2p_{3/2}$	4.93 ± 0.08	5.5
$2p_{1/2}$	3.26 ± 0.07	3.5
$1f_{5/2}$	≤1.8	1.9
$1g_{9/2}$	<1.7	...

[a] For definition, see text.

The spread of the $E^a_{1,1/2}$ and $E^a_{1,3/2}$ around the respective E' values is 1.5 to 2 MeV for Ca^{47}. Similar spreads were found for Ca^{41} (Ref. 16) and for Ti^{51} (Ref. 21). Thus, with regard to the strength of residual interactions in the $2p$-states, Ca^{47}, Ti^{51}, and Ca^{41} seem to be fairly similar, whereas Ca^{49} shows considerably less, if any, such strength. The similarity between Ca^{47} and Ti^{51} is not surprising, since relative to the Ca^{48} core the Ca^{47} p states are $(f_{7/2})^{-2}(p)^1$ neutron states, and the Ti^{51} p states are $_\pi(f_{7/2})^2{}_\nu(p)^1$ states (π standing for proton and ν for neutron), and both have $T=\frac{7}{2}$. The fact that Ca^{41} falls into line with Ca^{47} and Ti^{51} rather than Ca^{49} is more remarkable and throws further doubt on the inertness of the Ca^{40} core.

A comparison with other $N=27$ nuclei (Ti^{49}, Cr^{51}, and Fe^{53}) would be in place, but so far no high-resolution (d,p) data with DW analysis have been published for these nuclei.

2. Ground-State Q Value

Inside the framework of the seniority coupling scheme of a pure $(f_{7/2})^n$ configuration, a certain functional relation exists between the binding energies of the $(f_{7/2})^n$ ground states for $1\leqslant n\leqslant 7$. This functional relation has three free parameters. Adjusting these parameters to give the best fit to experimental Ca binding energies (this fit does not include Ca^{47}), a mass difference between Ca^{46} and Ca^{47} is predicted, corresponding to a $Ca^{46}(d,p)$ ground-state Q value of 4.77 MeV.[22] The experimental value is 5.05 MeV. Deviations of this magnitude are encountered in other calcium Q values also. The more recent work by Ginnochio and French[23] employs wave functions which, in the calcium case, are identical to those in Ref. 22.

3. Comparison with Other Experiments

The only two experiments so far reported on Ca^{47} are the decay scheme work of Ref. 1 and the Ca^{48} (p,d) experiment of Ref. 2. The present experiment, as well as the pickup experiment, agree on the character of the Ca^{47} ground state (see above). All three experiments place a level at 2.01 MeV with a probable spin of $\frac{3}{2}$. The decay work suggests positive parity, whereas the reaction works determine the parity as definitely negative. Provided that the same level is excited in all three experiments, the result of the reaction works probably is the more definitive.

All three experiments place levels close to 2.6 MeV. One level is seen in the decay scheme work probably of spin $\frac{3}{2}$. One transition is observed with $l_n=0$ and 2 in the (p,d) experiment. Two levels, one at 2.579 MeV and one at 2.606 MeV of $l_n=0$ character, are seen in the

[19] B. L. Cohen, R. H. Fulmer, A. L. McCarthy, and P. Mukherjee, Rev. Mod. Phys. **35**, 332 (1963).
[20] E. Kashy, A. Sperduto, H. A. Enge and W. W. Buechner, Phys. Rev. **135**, B865 (1964).
[21] P. D. Barnes, C. K. Bockelman, O. Hansen, and A. Sperduto, Phys. Rev. **136**, B438 (1964).
[22] A. de-Shalit and I. Talmi, *Nuclear Shell Theory* (Academic Press Inc., New York, 1963).
[23] J. N. Ginnochio and J. B. French, Phys. Letters **7**, 137 (1963).

present experiment. All data are consistent with the 2.579-MeV state being a $_p(1d_{3/2})^{-1}$ state relative to the Ca^{48} core and the 2.606-MeV state being a $\frac{1}{2}^+$ level also of hole character.

The fact is that the $_p(d_{3/2})^{-1}$ state is not (or only very weakly) excited in stripping points to a difference of the structure of the Ca^{46} and the Ca^{42} ground states, since in the Ca^{42} case at least one low-excitation (d,p) transition with $l_n=2$ to Ca^{43} was observed with appreciable strength.[24] Also, the low-excitation $l_n=0$ strength from $Ca^{46}(d,p)$ is less than that observed from $Ca^{42}(d,p)$ or $Ca^{40}(d,p)$ (Ref. 16). No such low-excitation transitions with $l_n=0$ or $l_n=2$ were found from Ca^{48} (Ref. 20). It may therefore be inferred that the (s,d) shell is more closely filled in the Ca^{48} and Ca^{46} cases than in the Ca^{40} and Ca^{42} cases; that is, $Ca^{48}(0)$ probably better represents a double-magic core than does $Ca^{40}(0)$ (see also Sec. III.1).

In Fig. 7 the level schemes for the three $N=27$ nuclei that may be reached through (d,p) reactions are shown. (The data are taken from Refs. 11, 25, and 26.)

It is apparent that the level density in Ti^{49} and Cr^{51} is considerably larger than in Ca^{47}. We interpret this effect as being due to the extra degrees of freedom associated with excited proton configurations avialable in the Ti and Cr cases, but apparently not in the Ca case.

Also conspicuous is the decrease in excitation energy of the first and second strong (d,p) $l_n=1$ states (indicated in the figure) when going from $Z=20$ to $Z=24$. This could indicate that the unperturbed single-particle energies $E'_{1,3/2}$ and $E'_{3,7/2}$ differ less from each other in Cr than in Ca, but such an effect could also be caused by a larger fractionation of the p strength in Cr than in Ca. The latter explanation would follow naturally from considering the excited proton degrees of freedom in Ti and Cr. The available deuteron stripping data on Ti^{48} and Cr^{50} (Refs. 25 and 26) are not detailed enough to select one of the two above explanations.

ACKNOWLEDGMENTS

It is our pleasant duty to acknowledge the support and hospitality of Dr. S. Hinds and Dr. R. Middleton of the Aldermaston Tandem Accelerator Laboratory in England. We are grateful to Dr. H. R. Blieden for his assistance in the early parts of this experiment. We should like to express our gratitude to Dr. G. R. Satchler and to Professor B. R. Mottelson for stimulating discussions. R. M. Drisko kindly made available the DW code JULIE. We owe special thanks to Miss Sara Lindström who carefully scanned the nuclear-track plates and who prepared part of the figures for this report.

[24] C. K. Bockelman, C. M. Braams, C. P. Browne, W. W. Buechner, R. R. Sharp and A. Sperduto, Phys. Rev. **107**, 176 (1957).
[25] B. Zeidman, J. L. Yntema, and B. J. Raz, Phys. Rev. **120**, 1723 (1960).
[26] L. H. T. Rietjens, O. M. Bilaniuk, and M. H. Macfarlane, Phys. Rev. **120**, 527 (1960).